14th Annual (International) Mechanical Engineering Conference – May 2006
Isfahan University of Technology, Isfahan, Iran

NON-LINEAR BENDING RESPONSE OF FUNCTIONALLY GRADED BEAMS UNDER TRANSVERSE LOADS

M. Tahani[1], M. A. Torabizadeh[2], A. Fereidoon[3]
[1] **Department of Mechanical Engineering, Ferdowsi University of Mashhad, Mashhad, Iran**
[2,3] **Department of Mechanical Engineering, University of Semnan, Semnan, Iran**

mtahani@ferdowsi.um.ac.ir (M. Tahani)

Abstract

In this study, an analytical method is developed to analyze analytically displacements and stresses in a functionally graded composite beam subjected to transverse load. Assuming the functionally graded beam has nonhomogeneous mechanical properties in the thickness direction, the displacements and stresses of the beam are obtained based on a first-order shear deformation beam theory (FSDBT). The non-linear strain-displacement relations in the von Kármán sense are used to study the effect of geometric non-linearity. Equilibrium equations are obtained by using the principle of minimum total potential energy and solved exactly. The results obtained from this method are compared with the finite element solution done by ANSYS. Numerical results of the first-order linear and non-linear theories are presented to show the effects of using FGMs instead of classical layered composites on the deflections and stresses.

Keywords: Functionally graded beam - Geometric non-linearity – Transverse load.

Introduction

The concept of functionally graded materials (FGMs), i.e. composites with smoothly varying constitutive properties, was first suggested by Niino and coworkers at the National Aerospace Laboratory in Japan [1]. Functionally graded materials constitute a new class of heterogeneous materials that allow for spatial optimization of properties in one or more dimensions in a defined geometry [2]. Functionally graded materials are characterized by a continuously changing property due to a continuous change in composition, in morphology, in microstructure or in crystal structure from one surface of the material to the other [3]. The original idea was to manufacture super-heat-resistant components for use in the engines and airframe of supersonic plane, combining the heat resistance of ceramics with the structural properties of metals [4].
Compared with classical laminated composite materials, functionally graded materials provide superior thermo-mechanical performances under given loading circumstances [5]. In classical laminated composites, the sudden change in material properties across the interface between discrete materials can result in large interlaminar stresses leading to delamination. Furthermore, large plastic deformations at the interfaces may trigger the initiation and propagation of cracks in the material. One way to overcome these effects is to use functionally graded materials [6-7]. FGMs can be used to improve fracture toughness of machine tools, wear resistance and oxidation resistance of high temperature aerospace and automotive components, and ballistic efficiency of light weight armor materials [8].
With the advent of FGMs there has been a renewed interest in inhomogeneous elasticity. For example Tanaka et al. [9, 10] designed property profiles for FGMs to reduce the thermal stresses. Reddy [11] has presented solutions for rectangular plates based on the third-order shear deformation plate theory. The formulation accounted for the thermo-mechanical coupling, time dependency, and the von Kármán-type geometric non-linearity. Reiter et al. [12] and Reiter and Dvorak [13] performed detailed finite

1-Assistant professor
2- M.S. student
3- Assistant professor

element studies of discrete models containing simulated skeletal and particulate microstructures. They compared their results with those computed from homogenized models in which effective properties were derived by the Mori-Tanaka and the self-consistent methods. Sankar [14] obtained an elasticity solution for a functionally graded beam subjected to transverse loads. Praveen and Reddy [15] investigated the response of functionally graded ceramic-metal plates using a plate finite element that accounts for the transverse shear strains, rotary inertia and moderately large rotations in the von Kármán sense. Yang and Shen [16] analyzed the non-linear bending and postbuckling behaviors of functionally graded rectangular plates subjected to combined action of transverse and in-plane loads and without or resting on an elastic foundation by using a semi-analytical approach.

In this paper, a first-order shear deformation beam theory (FSDBT) is used to analyze displacements and stresses in beams made of functionally graded materials. The non-linear strain-displacement relations are used to study the effect of geometric non-linearity on displacements and stresses of the beams. The equilibrium equations are solved exactly for various loading conditions. The results are compared with those obtained from the finite element solution. Finally, effects of considering geometric non-linearity and also effects of using FGMs instead of convensional bi-material (ceramic-metal) layered composites on deflections and stresses are determined.

Material property estimation approach

There are some approximations that can be used to model the variation of material properties in a FGM. One such variation is a power-law distribution. According to this estimation method, a generic material property $p(z)$ at a point z in FGMs is approximated by:

$$p(z) = (p_t - p_b)\left(\frac{z}{h} + \frac{1}{2}\right)^n + p_b \tag{1}$$

where p_t and p_b are the properties of the material at the top and bottom surfaces of the beam, respectively, h is the total thickness of the beam and n is the value of the gradient exponent that controls the compositional gradient, either linear or non-linear. Here we assume that moduli E and G vary according to Eq. (1) and the Poisson's ratio ν is assumed to be a constant. Distribution of volume fraction through the thickness of the beam for various values of the power-law index n is shown in Fig. 1.

Theoretical formulation

Consider a functionally graded beam shown in Fig. 2. It is to be noted that the origin of the coordinate is at the mid-plane of the beam. The length of the beam is L, its total thickness is h, and its width is b. The bottom surface of the beam ($z = -h/2$) is subjected to a normal traction. That is:

$$\sigma_{zz}(x, -h/2) = -q(x) \tag{2}$$

It is assumed that the upper surface ($z = h/2$) is completely free of tractions, and the lower surface is free of shear tractions.

Displacement field and strains

Here a first-order shear deformation plate theory is used to derive first-order shear deformation beam theory. The displacement field is assumed as:

$$\begin{aligned} u(x,y,z) &= u_0(x,y) + z\psi_x(x,y) \\ v(x,y,z) &= v_0(x,y) + z\psi_x(x,y) \\ w(x,y,z) &= w(x,y) \end{aligned} \tag{3}$$

where u_0, v_0 and w denote the displacements of a point on the middle plane of the plate ($z = 0$). Also ψ_x and ψ_y are unknown functions which denote rotations of the cross-section about y and x axes, respectively. In the present study we wish to investigate the effect of geometric non-linearity on the response quantities. Therefore, the von Kármán-type of geometric non-linearity is taken into consideration in the strain-displacement relations. Substituting Eqs. (3) in the appropriate strain-displacement relations results in:

$$\begin{aligned} &\varepsilon_x = \varepsilon_x^0 + zk_x, \quad \varepsilon_y = \varepsilon_y^0 + zk_y, \quad \varepsilon_z = 0 \\ &\gamma_{xy} = \gamma_{xy}^0 + zk_{xy}, \quad \gamma_{xz} = \gamma_{xz}^0, \quad \gamma_{yz} = \gamma_{yz}^0 \end{aligned} \tag{4}$$

where

$$\begin{aligned} &\varepsilon_x^0 = \frac{\partial u_0}{\partial x} + \frac{1}{2}\left(\frac{\partial w}{\partial x}\right)^2, \quad k_x = \frac{\partial \psi_x}{\partial x} \\ &\varepsilon_y^0 = \frac{\partial v_0}{\partial y} + \frac{1}{2}\left(\frac{\partial w}{\partial y}\right)^2, \quad k_y = \frac{\partial \psi_y}{\partial y} \\ &\gamma_{yz}^0 = \psi_y + \frac{\partial w}{\partial y}, \quad \gamma_{xz}^0 = \psi_x + \frac{\partial w}{\partial x} \\ &\gamma_{xy}^0 = \frac{\partial u_0}{\partial y} + \frac{\partial v_0}{\partial x} + \frac{\partial w}{\partial x}\frac{\partial w}{\partial y} \\ &k_{xy} = \frac{\partial \psi_x}{\partial y} + \frac{\partial \psi_y}{\partial x} \end{aligned} \tag{5}$$

Plate equilibrium equations

Using the principle of minimum total potential energy, the equilibrium equations can be shown to be:

$$\begin{aligned}
&\delta u_0 : \frac{\partial N_x}{\partial x} + \frac{\partial N_{xy}}{\partial y} = 0 \\
&\delta v_0 : \frac{\partial N_{xy}}{\partial x} + \frac{\partial N_y}{\partial y} = 0 \\
&\delta \psi_x : \frac{\partial M_x}{\partial x} + \frac{\partial M_{xy}}{\partial y} - Q_x = 0 \\
&\delta \psi_y : \frac{\partial M_{xy}}{\partial x} + \frac{\partial M_y}{\partial y} - Q_y = 0 \\
&\delta w : \frac{\partial Q_x}{\partial x} + \frac{\partial Q_y}{\partial y} + \mathrm{N}(w) + q(x,y) = 0
\end{aligned} \tag{6}$$

where

$$\begin{aligned}
\mathrm{N}(w) = &\frac{\partial}{\partial x}\left(N_x \frac{\partial w}{\partial x} + N_{xy} \frac{\partial w}{\partial y} \right) \\
&+ \frac{\partial}{\partial y}\left(N_{xy} \frac{\partial w}{\partial x} + N_y \frac{\partial w}{\partial y} \right)
\end{aligned} \tag{7}$$

and $q(x,y)$ is the transverse load that is applied on the bottom surface of the plate. Also the force and moment resultants are defined as:

$$\begin{aligned}
&\left(N_x, N_y, N_{xy}\right) = \int_{-h/2}^{h/2} (\sigma_x, \sigma_y, \sigma_{xy}) dz \\
&\left(M_x, M_y, M_{xy}\right) = \int_{-h/2}^{h/2} (\sigma_x, \sigma_y, \sigma_{xy}) z dz \\
&\left(Q_x, Q_y\right) = \int_{-h/2}^{h/2} (\sigma_{xz}, \sigma_{yz}) dz
\end{aligned} \tag{8}$$

The primary variables of the theory are:

$$u_0,\ v_0,\ \psi_x,\ \psi_y,\ w \tag{9}$$

Also the secondary variables are;

at $x = \pm L/2$:

$$N_x, N_{xy}, M_x, M_{xy}, N_x \frac{\partial w}{\partial x} + N_{xy} \frac{\partial w}{\partial y} + Q_x \tag{10a}$$

at $y = \pm b/2$:

$$N_{xy}, N_y, M_{xy}, M_y, N_{xy} \frac{\partial w}{\partial x} + N_y \frac{\partial w}{\partial y} + Q_y \tag{10b}$$

The linear constitutive relations are given by:

$$\begin{aligned}
&\begin{Bmatrix} \sigma_x \\ \sigma_y \\ \sigma_{xy} \end{Bmatrix} = \begin{bmatrix} Q_{11} & Q_{12} & 0 \\ Q_{12} & Q_{22} & 0 \\ 0 & 0 & Q_{66} \end{bmatrix} \begin{Bmatrix} \varepsilon_x \\ \varepsilon_y \\ \gamma_{xy} \end{Bmatrix} \\
&\begin{Bmatrix} \sigma_{yz} \\ \sigma_{xz} \end{Bmatrix} = \begin{bmatrix} C_{44} & 0 \\ 0 & C_{55} \end{bmatrix} \begin{Bmatrix} \gamma_{yz} \\ \gamma_{xz} \end{Bmatrix}
\end{aligned} \tag{11}$$

where

$$\begin{aligned}
&Q_{11} = Q_{22} = \frac{E(z)}{1-\nu^2} \\
&Q_{12} = \frac{\nu E(z)}{1-\nu^2} \\
&C_{44} = C_{55} = Q_{66} = \frac{E(z)}{2(1+\nu)} = G
\end{aligned} \tag{12}$$

Upon substitution of Eqs. (4) into Eqs. (11) and the subsequent results into Eqs. (8), the force and moment resultants will be obtained which can be presented as follows:

$$\begin{Bmatrix} N_x \\ N_y \\ N_{xy} \end{Bmatrix} = \begin{bmatrix} A_{11} & A_{12} & 0 \\ A_{12} & A_{22} & 0 \\ 0 & 0 & A_{66} \end{bmatrix} \begin{Bmatrix} \varepsilon_x^0 \\ \varepsilon_y^0 \\ \gamma_{xy}^0 \end{Bmatrix} + \begin{bmatrix} B_{11} & B_{12} & 0 \\ B_{12} & B_{22} & 0 \\ 0 & 0 & B_{66} \end{bmatrix} \begin{Bmatrix} k_x \\ k_y \\ k_{xy} \end{Bmatrix} \tag{13a}$$

$$\begin{Bmatrix} M_x \\ M_y \\ M_{xy} \end{Bmatrix} = \begin{bmatrix} B_{11} & B_{12} & 0 \\ B_{12} & B_{22} & 0 \\ 0 & 0 & B_{66} \end{bmatrix} \begin{Bmatrix} \varepsilon_x^0 \\ \varepsilon_y^0 \\ \gamma_{xy}^0 \end{Bmatrix} + \begin{bmatrix} D_{11} & D_{12} & 0 \\ D_{12} & D_{22} & 0 \\ 0 & 0 & D_{66} \end{bmatrix} \begin{Bmatrix} k_x \\ k_y \\ k_{xy} \end{Bmatrix} \tag{13b}$$

$$\begin{Bmatrix} Q_y \\ Q_x \end{Bmatrix} = k^2 \begin{bmatrix} A_{44} & 0 \\ 0 & A_{55} \end{bmatrix} \begin{Bmatrix} \gamma_{yz} \\ \gamma_{xz} \end{Bmatrix} \tag{13c}$$

where

$$\begin{aligned}
&(A_{ij}, B_{ij}, D_{ij}) = \int_{-h/2}^{h/2} Q_{ij} (1, z, z^2) dz \quad (i, j = 1,2,6) \\
&A_{ij} = \int_{-h/2}^{h/2} C_{ij} dz \quad (i, j = 4,5)
\end{aligned} \tag{14}$$

and $k^2 (= 5/6)$ is the shear correction factor.

Beam equilibrium equations

Next, in order to derive the beam theroy it is assumed that:

$$N_y = M_y = 0 \tag{15}$$

By imposing the assumtions (15) in Eqs. (13a) and (13b) resuls in:

$$\begin{Bmatrix} N_x \\ M_x \end{Bmatrix} = \begin{bmatrix} \bar{A}_{11} & \bar{B}_{11} \\ \bar{B}_{11} & \bar{D}_{11} \end{bmatrix} \begin{Bmatrix} \varepsilon_x^0 \\ k_x \end{Bmatrix} \tag{16}$$

where

$$\begin{bmatrix} \bar{A}_{11} & \bar{B}_{11} \\ \bar{B}_{11} & \bar{D}_{11} \end{bmatrix} = \begin{bmatrix} A_{11} & B_{11} \\ B_{11} & D_{11} \end{bmatrix} - \begin{bmatrix} A_{12} & B_{12} \\ B_{12} & D_{12} \end{bmatrix} \begin{bmatrix} A_{22} & B_{22} \\ B_{22} & D_{22} \end{bmatrix}^{-1} \begin{bmatrix} A_{12} & B_{12} \\ B_{12} & D_{12} \end{bmatrix} \quad (17)$$

It is also assumed that all the force and moment resultants are functions of coordinate *x* only. Hence, Eqs. (6) are simplified as follows:

$$\delta u_0 : \frac{dN_x}{dx} = 0 \quad (18a)$$

$$\delta v_0 : \frac{dN_{xy}}{dx} = 0 \quad (18b)$$

$$\delta \psi_x : \frac{dM_x}{dx} - Q_x = 0 \quad (18c)$$

$$\delta \psi_y : \frac{dM_{xy}}{dx} - Q_y = 0 \quad (18d)$$

$$\delta w : \frac{dQ_x}{dx} + \frac{d}{dx}\left(N_x \frac{dw}{dx} \right) + q(x) = 0 \quad (18e)$$

where $q(x)$ is the transverse load on the bottom surface of the beam as shown in Fig. 2.

Exact solutions

In this section a beam subjected to a uniform transverse load on its bottom surface is considered. The boundary conditions of the beam at $x = \pm L/2$ are assumed to be the same. In order to obtain the exact solutions of equilibrium equations (18), Eq. (18a) is integrated with respect to *x* to yield:

$$N_x = N_x^0 \quad \text{or} \quad \bar{A}_{11}\varepsilon_x^0 + \bar{B}_{11}k_x = N_x^0 \quad (19)$$

where N_x^0 is a constant of integration. Next we solve Eq. (11) to obtain:

$$\varepsilon_x^0 = \frac{1}{\bar{A}_{11}}\left(N_x^0 - \bar{B}_{11}k_x \right) \quad (20)$$

With (20), Eqs. (5) and (13), with $\partial/\partial y = 0$, are substituted into Eqs. (18) to yield:

$$u_0' + \frac{1}{2}(w')^2 = \frac{1}{\bar{A}_{11}}(N_x^0 - \bar{B}_{11}\psi_x') \quad (21a)$$

$$A_{66}v_0'' + B_{66}\psi_y'' = 0 \quad (21b)$$

$$\left(\bar{D}_{11} - \frac{\bar{B}_{11}^2}{\bar{A}_{11}} \right)\psi_x'' - k^2 A_{55}(\psi_x + w') = 0 \quad (21c)$$

$$B_{66}v_0'' + D_{66}\psi_y'' - k^2 A_{44}\psi_y = 0 \quad (21d)$$

$$k^2 A_{55}(\psi_x' + w'') + N_x^0 w'' = -q(x) \quad (21e)$$

where a prime indicates an ordinary derivative with respect to *x*. Eqs. (21) are five linear ordinary differential equations with constant coefficients. It is noted that Eqs. (21b) and (21d) are both homogeneous and in terms of v_0 and ψ_y only. Since the corresponding boundary conditions (i.e., $v_0 = 0$ or $N_{xy} = 0$ and $\psi_y = 0$ or $M_{xy} = 0$) are all homogeneous and in terms of v_0 and ψ_y only, the solution of Eqs. (21b) and (21d) is only a trivial one. That is:

$$v_0 = \psi_y = 0 \quad (22)$$

Now it remains to solve Eqs. (21a), (21c) and (21e). These equations can be solved analytically for any sets of boundary conditions in terms of the unknown constant N_x^0. After solving these equations in terms of N_x^0, we note that from symmetry we have:

$$u_0 = 0 \quad \text{at} \quad x = \pm L/2 \quad (23)$$

This will allow us to find N_x^0 in a trial and error process. Towards this end, we note that integrating Eq. (21a) once from 0 to $L/2$ and then from $-L/2$ to 0 results in:

$$u_0\left(\frac{L}{2}\right) = u_0(0) - \int_0^{L/2}\left[\frac{\bar{B}_{11}\psi_x'}{\bar{A}_{11}} + \frac{(w')^2}{2} \right]dx + \frac{N_x^0 L}{2\bar{A}_{11}} \quad (24a)$$

$$u_0\left(-\frac{L}{2}\right) = u_0(0) - \int_0^{-L/2}\left[\frac{\bar{B}_{11}\psi_x'}{\bar{A}_{11}} + \frac{(w')^2}{2} \right]dx - \frac{N_x^0 L}{2\bar{A}_{11}} \quad (24b)$$

Clearly, because of symmetry, the integral in (24b) is negative of the integral in (24a). On the other hand, we have:

$$u_0(L/2) = u_0(-L/2) = u_0(0) = 0 \quad (25)$$

Therefore, we conclude that:

$$\int_0^{L/2}\left[\frac{\bar{B}_{11}\psi_x'}{\bar{A}_{11}} + \frac{(w')^2}{2} \right]dx = \frac{N_x^0 L}{2\bar{A}_{11}} \quad (26)$$

Finally, by making the solutions of the Eqs. (21a), (21c) and (21e) to satisfy (26) in a trial and error process, we will obtain the exact value of N_x^0.

Results and discussion

Here we present exact results for a representative clamped supported beam which its bottom surface ($z = -h/2$) is rich of Aluminum and the top surface ($z = h/2$) is rich of Zirconia (see Fig. 3). Boundary conditions of the clamped-clamped beam are assumed as:

$$u_0 = \psi_x = w = 0 \quad (27)$$

It is also assumed that the beam is subjected to a uniform transverse load (i.e., $q(x)=q_0$). Furthermore, the length-to-thickness ratio (i.e., *L/h*) is assumed to be 15 in all numerical examples. The mechanical properties of the constituents are as follow:

$$E_m = 70\,\text{GPa}, \quad E_c = 151\,\text{GPa}$$
$$\nu_m = 0.3, \qquad \nu_c = 0.3 \tag{28}$$

where *m* and *c* indicate metal (i.e. Aluminum) and ceramic (i.e. Zirconia), respectively. In the numerical results the various non-dimensionalized parameters used are:

Length: *x/L*
Center deflection: *w/h*
Longitudinal stress: $\bar{\sigma}_x = \left(\sigma_x h / q_0 L\right)$ (29)
Load parameter: $\bar{q} = \left(q_0 L^4 / E_m h^4\right)$

where q_0 denotes the intensity of the applied uniform load.

It is noted that for brevity all the numerical examples presented in what follows are for a FG beam with power-law index *n*=3 subjected to the load $\bar{q} = 36.16$.

In order to test the correctness and accuracy of the present method, bending of the FG beam under uniform transverse load is considered. The assessment of the accuracy of the present method is obtained by comparison the results with those obtained by utilizing the finite element package of ANSYS. The clamped supported beam has been modeled in ANSYS by using three-dimensional 8-node structural solid elements. In order to model the FG beam in ANSYS, the graded layer is discretized into several homogenized sublayers of the equal thickness with different matrial properties obtained from Eq. (1). Also the mesh is refined till no significant change in displacements and stresses are obtained. Figs. 4 and 5 illustrate the distributions of non-dimensionalized longitudinal deformation u_0/L and transverse deflection w/h, respectively, along the middle plane of the beam. Also variation of longitudinal stress $\bar{\sigma}_x$ along the bottom surface of the beam is shown in Fig. 6. It is observed from these figures that the present results agree well with those obtained from finite element method.

Fig. 7 presents the variation of the center deflection of the beam versus the load parameter $\bar{q}$. It is seen that for the maximum deflections greater than 0.3*h* a non-linear solution is required.

Figs. 8 and 9 show the effect of geometric non-linearity on the distributions of non-dimensionalized transverse deflection along the middle plane and non-dimensionalized longitudinal stress along the bottom surface of the beam, respectively. It is seen that both the maximum deflection and normal stress in non-linear analysis are smaller in magnitude in compared with linear analysis.

Finally, it is intended here to study the effects of using a FG beam as a substitue for a layered bi-material composite beam. To this end, a bi-material beam where the transition is made smooth (see Fig. 3) and a two-layered equal thickness composite beam that the bottom and top layers are made of Aluminium and Zirconia (see Fig. 10), respectively, are considered. Distributions of non-dimensionalized transverse deflection and longitudinal stress in Aluminium and Zirconia beams and also in the FG and classical layered composite beams are illustrated in Figs. 11 and 12. The transverse deflection are generated for FG beams with the power-law indexes 0.5, 1, 3 and 5. It is observd that by using a FG beam as an alternative for a classical two-layered composite beam both the transverse deflection and maximum longitudinal stress could be reduced.

Conclusions

An analytical solution is obtained for functionally gradient beams subjected to uniform transverse loadings. The formulation accounts for the von Kármán-type geometric non-linearity. The Poisson ratio is assumed to be a constant, and the Young's modulus is assumed to vary according to a power-law distribution in terms of the volume fractions of the constituents. A first-order shear deformation beam theory is used to analyze displacements and stresses in beams made of functionally graded materials. The results are obtained for the power-law index *n*=3 and compared with the finite element solution. It is found that the stresses and displacements in FG beams decrease about 30% in compared with classical two-layered composite beams made of Aluminum-Zirconia. Also the effect of geometric non-linearity on stresses and displacements is determined, which significantly affect the response of a functionally graded beam under mechanical loads.

References

1- M. Koizumi, "The Concept of FGM," Ceramic Transactions, 1993, pp. 3-10.
2- S.B. Binder, "Thermo-Elastic Analysis of Functionally Graded Materials Using Voronoi Elements," Materials Science and Engineering A315, 2001, pp. 136-146
3- L. Shaw, "Thermal Residual Stresses in Plates and Coatings Composed of Multi-Layered and Functionally Graded Materials," 1997, pp. 59-68.
4- F. Rooney, M. Ferrari, "Tension, Bending, and Flexure of Functionally Graded Cylinders,"

International Journal of Solids and Structures, Vol. 38, 2001, pp. 413-421.

5- J.R. Cho, D.Y. Ha, "Averaging and Finite Element Discretization Approaches in the Numerical Analysis of Functionally Graded Materials," Materials Science and Engineering A302, 2001, pp.187-196.

6- S. Senthil, R.C. Batra, "Exact Solution for Thermo-Elastic Deformations of Functionally Graded Thick Rectangular Plates," AIAA Journal, Vol. 40, No. 7, 2002.

7- Y. Fukui, "Fundamental Investigation of Functionally Gradient Materials Manufacturing System Using Centrifugal Force," JSME International Journal Series III, Vol. 34, No. 1, 1991, pp. 144-148.

8- Li. Jiang, "Thermoelastic Behavior of Composites with Functionally Graded Interphase," International Journal of Solids and Structures, Vol. 37, 2000, pp.5579-5597.

9- K. Tanaka, Y. Tanaka, K. Enomoto., V.F. Poterasu, Y. Sugano, "Design of Thermoelastic Materials Using Direct Sensitivity and Optimization Methods," Computer Methods in Applied Mechanics and Engineering, Vol. 106, No.1-2, 1993, pp.271-284.

10- K. Tanaka, Y. Tanaka, H. Watanabe, V.F. Poterasu, Y. Sugano, "An Improved Solution to Thermoelastic Material Design in Functionally Gradient Materials," Computer Methods in Applied Mechanics and Engineering, Vol. 109, No. 3-4, 1993, pp. 377-389.

11- J.N. Reddy, "Analysis of Functionally Graded Plates," International Journal for Numerical Methods in Engineering, Vol. 47, 2000, pp. 663-684.

12- T. Reiter, G.J. Dvorak, V. Trergaard, "Micromechanical Models for Graded Composite Materials," Journal of the Mechanics and Physics of Solids, Vol. 45, No. 8, 1997, pp. 1281-1302.

13- T. Reiter, G.J. Dvorak, "Micromechanical Modeling of Functionally Graded Materials," IUTAM Symposium a Transformation Problems in Composite and Active Materials, London, 1997, pp. 173-184.

14- B.V. Sankar, "An Elasticity Solution for Functionally Graded Beams," Composite Science and Technology, Vol. 61, 2001, pp. 689-696.

15- G.N. Praveen, J.N. Reddy, "Nonlinear Transient Thermoelastic Analysis of Functionally Graded Ceramic-Metal Plates," Internationa Journal of Solids and Structures, Vol. 35, No. 33, 1998, pp. 4457-4476.

16- J. Yang, H.-S. Shen, "Non-Linear Analysis of Functionally Graded Plates Under Transverse and In-Plane Loads," International Journal of Non-Linear Mechanics, Vol. 38, 2003, pp. 467-482.

Figures and Graphs

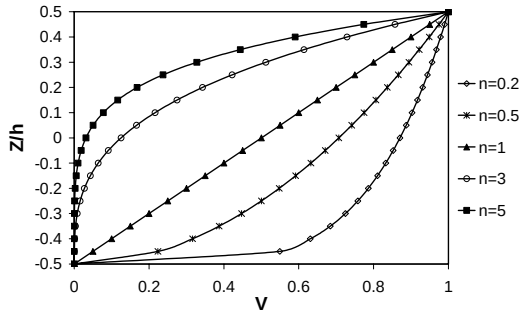

Fig. 1. Distribution of volume fraction of the ceramic phase through beam thickness for various values of the power-law index *n*

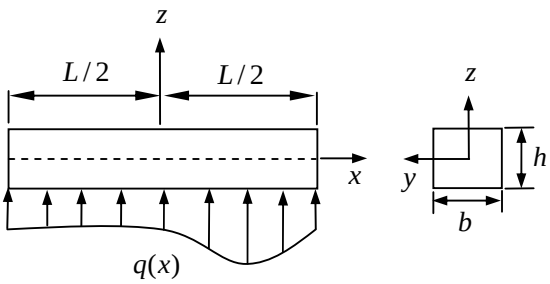

Fig. 2. A FG beam subjected to a transverse load

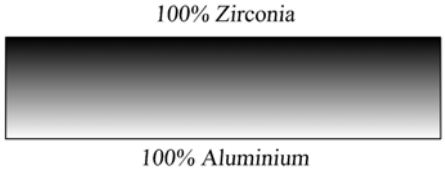

Fig. 3. A FG Aluminum-Zirconia beam

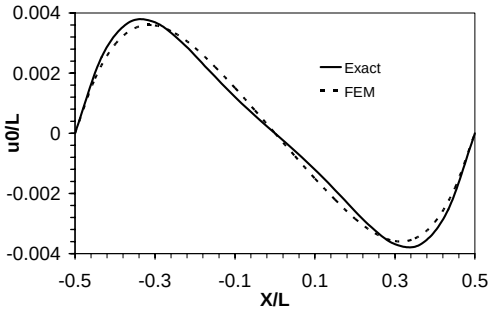

Fig. 4. Distribution of longitudinal deformation along the middle plane of the beam

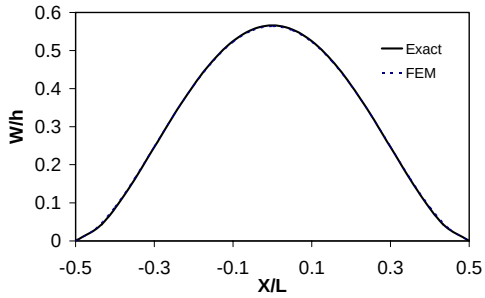

Fig. 5. Distribution of transverse deflection w/h along the middle plane of the beam

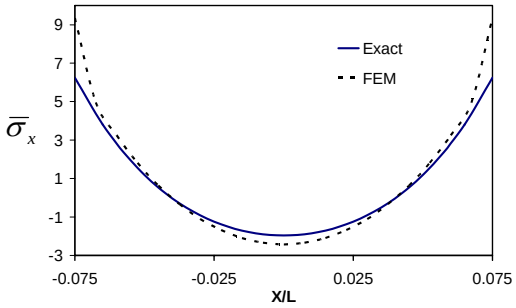

Fig. 6. Distribution of longitudinal stress $\overline{\sigma}_x$ at the bottom surface of the beam

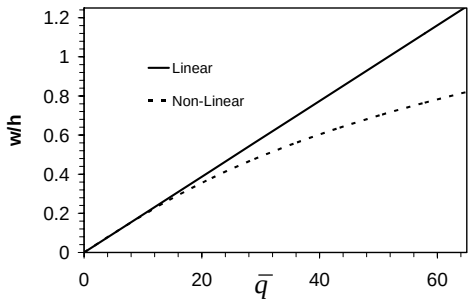

Fig. 7. Vriation of center deflection of the beam versus the load parameter $\overline{q}$

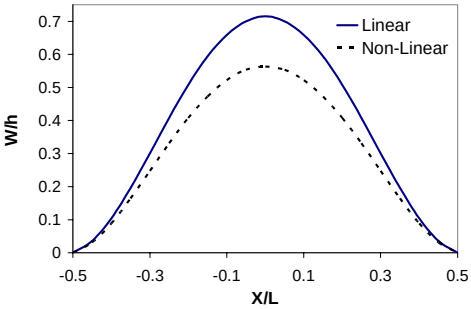

Fig. 8. Distribution of linear and non-linear transverse deflection w/h along the middle plane of the beam

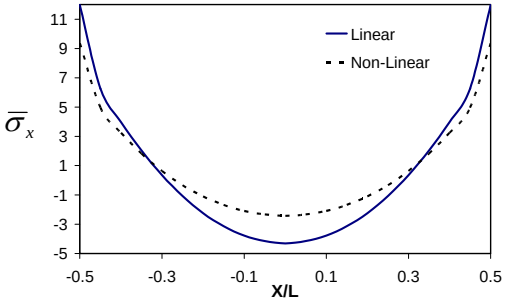

Fig. 9. Distribution of longitudinal stress $\overline{\sigma}_x$ along the bottom surface of the beam for linear and non-linear analyses

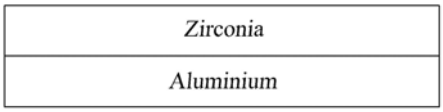

Fig. 10. Classical layered composite made of equal thickness Aluminium and Zirconia layers

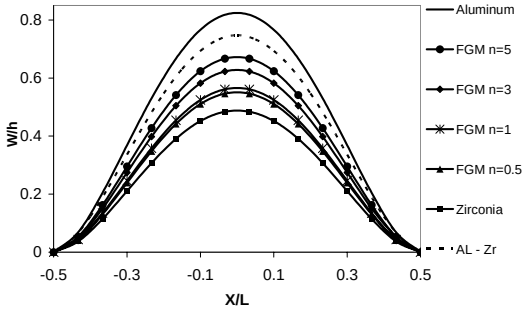

Fig. 11. Distributions of transverse deflection w/h along the middle plane of Aluminium, Zirconia, FG and classical layered composite beams

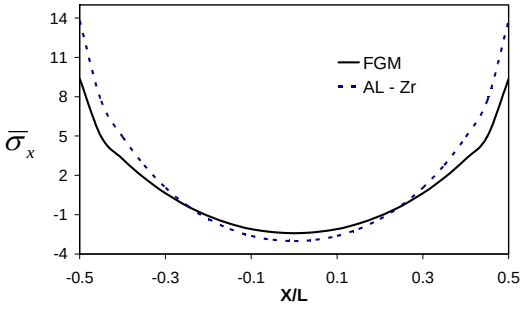

Fig. 12. Distributions of longitudinal stress $\overline{\sigma}_x$ along the bottom surface of Aluminium, Zirconia, FG and classical layered composite beams